Langmuir

Letter

pubs.acs.org/Langmuir

# Nanostructure of Complexes Between Cationic Lipids and an Oppositely Charged Polyelectrolyte

Sharon Golan and Yeshayahu Talmon*

Department of Chemical Engineering, Technion-Israel Institute of Technology, Haifa 32000, Israel

**ABSTRACT:** The morphology of aqueous solutions of polyelectrolytes and oppositely charged lipids is the subject of extensive colloid science research, because of their application in industry and medicine, the latter especially for gene therapy. In this work, we show that complexes of two different cationic lipids with the polyelectrolyte sodium poly(acrylic acid), PAA, share similar morphology with the complexes of those lipids with nucleic acids, implying a broader and universal packing phenomenon. We characterized by direct-imaging cryogenic-temperature transmission electron microscopy (cryo-TEM), dynamic light scattering (DLS), and zeta ($\zeta$)-potential two cationic lipids, 1,2-dioleoyl-3-trimethylammonium-propane (DOTAP) and bis(11-ferrocenylundecyl) dimethylammonium bromide (BFDMA), which are used in gene transfection, at equivalent lipid/polyelectrolyte charge ratio. Our results revealed that, for both types of complexes, onion-like multilamellar nanostructures formed, which exhibited similar morphology as in complexes of DNA or oligonucleotides (lipoplexes), based on the same lipids. Our findings suggest that the onion-like packing may be energetically favorable for a wide range of polyelectrolyte-liposome systems, from oligonucleotides and DNA to PAA.

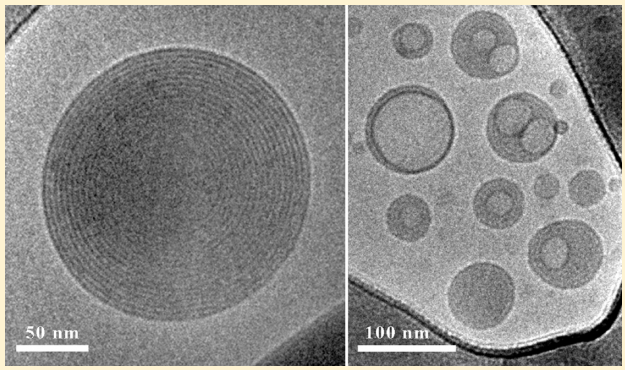


## INTRODUCTION

The morphology of complexes formed by amphiphiles and oppositely charged polymers have been widely studied,[1−6] especially in the case of positively charged lamellae-forming lipids, which have been shown to be attractive delivery carriers in biotechnology applications.[7−11] The interaction of lipids and oppositely charged polyelectrolytes depends on the electrostatic interactions between the lipid and the polymer, charge distribution on the lipid and the polymer, polymer branching, flexibility, and the solution conditions, i.e., type of medium, ionic strength, and pH. In the case of lamellae-forming surfactants and oppositely charged polyelectrolyte, the polymer is expected to enter into the water layers, and induce water swelling of the lamellar phase.[1,2,6]

Safinya[12] showed by high-resolution synchrotron small-angle X-ray scattering (SAXS) that cationic lipid and DNA complexes form multilamellar nanostructure ($L_\alpha^C$) composed of DNA monolayers sandwiched between two adjacent lipid bilayers, or inverted hexagonal phase ($H_{II}^C$), where the DNA is coated by lipid monolayers in a hexagonal lattice. Later, Weisman et al.[13] showed by cryo-TEM the detailed mechanism of the $L_\alpha^C$ phase formation. Antunes et al.[1] used cryo-TEM to characterize the structure of complexes between an overall net negatively charged cationic and anionic surfactant mixtures and cationic polyelectrolytes of different charge densities. They showed that the addition of a highly charged polycation to the surfactant solution caused extensive modifications to the vesicle structure of the surfactants, by inducing polygon shapes, and perforated patches in the vesicle membranes. Volodkin et al.[6] studied the interaction of anionic liposomes based on phosphocholine and the cationic linear poly(L-lysine) (PLL) using dynamic light scattering (DLS), electrorophoretic mobility, and differential scanning calorimetry (DSC). Their results suggested that the polymer interacts with the vesicle surface, and the lipid organization is not disturbed significantly.

Bordi et al. studied extensively the morphology and physicochemical properties of complexes between 1,2-dioleoyl-3-trimethylammonium-propane (DOTAP) and sodium poly(acrylic acid) (NaPAA).[14−18] They found that, as polyelectrolyte/lipid charge ratio increased, the aggregate size increased, until a maximum was reached near the isoelectric point (where the overall net charge in the electric double layer of the lipid/polyelectrolyte aggregates is zero). Further increase of the charge ratio reduced the aggregate size, until the aggregate size returned to the size of the original liposomes. They used staining and drying TEM to characterize the morphology nanostructures of these complexes. Their results showed that complexes appeared as clusters of cationic liposomes "glued" together by the polyelectrolyte, while maintaining their liposome integrity. However, that TEM methodology had been shown to be artifact laden.[19,20]

This literature review demonstrates that most studies concentrate on a specific type of lipid and polymer, and the results cannot be assumed for other complexes systems. Our

**Received:** October 19, 2011
**Revised:** December 21, 2011
**Published:** January 3, 2012





dx.doi.org/10.1021/la204095s | *Langmuir* 2012, 28, 1668−1672

study tries to address the question whether the morphology of these complexes may be a general phenomenon, independent of the type of the polymer.

In this letter, we report the nanostructure characterization of complexes between the polyelectrolyte NaPAA and two cationic lipids, DOTAP and reduced bis(11-ferrocenylundecyl)-dimethylammonium bromide (BFDMA, Figure 1), at lipid/

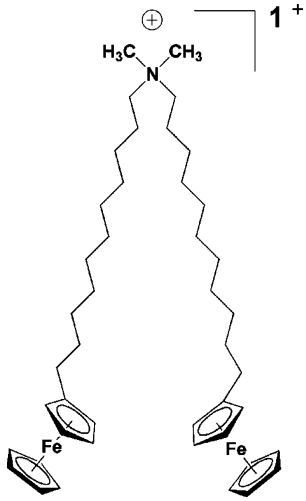


**Figure 1.** Chemical structure of reduced BFDMA.

polymer charge ratio of 1. Previously, we reported that these lipids form multilamellar onion-like nanostructures when complexed with nucleic acids.[11,13,22] Therefore, they are good candidates for the comparison of their morphological attributes with the very different polyelectrolyte PAA. We employed direct-imaging cryo-TEM with the complementary techniques DLS and $\zeta$-potential measurements. Cryo-TEM is a powerful characterization tool, which allows imaging of the sample in its original composition and state (i.e., without drying or addition of other components to the solution).[21] The complexes between the cationic liposomes and the anionic polymer exhibited multilamellar morphology, similar to the multilamellar morphology of these cationic lipids with nucleic acids.[7,8,10−12,22] Our results suggest a "proof of concept" of a general phenomenon that the addition of polyelectrolyte to oppositely charged lamellar forming lipids induces aggregation of multilamellar nanostructures, in which the polymer is sandwiched between two adjacent lipid bilayers.

## EXPERIMENTAL SECTION

The anionic polyelectrolyte NaPAA (average $M_W$ ~15 000) was purchased from Sigma-Aldrich. The cationic lipid DOTAP in chloroform was purchased from Avanti Polar Lipids, and reduced BFDMA was generously contributed by Professor Nicholas L. Abbott, University of Wisconsin, Madison. The chloroform of the original DOTAP solution was removed by a stream of nitrogen, and the dried lipid film was kept overnight in desiccator under vacuum. Then, 1 mM DOTAP was dispersed in a HEPES buffer (pH 7.2, 20 mM) and sonicated in a "cup-horn" sonicator (Heat Systems-Ultrasonic, Inc., New York) at 25 °C for about 30 min, until the dispersion clarified. BFDMA powder was dissolved in aqueous $Li_2SO_4$ (1 mM, pH 5), and sonicated in a bath sonicator for about 15 min, until the BFDMA was suspended in the solution (1 mM BFDMA). Dilute NaPAA solution was added to the 1 mM lipid solutions in appropriate amounts to produce lipid/polyelectrolyte charge ratio of 1. The dispersions were then incubated in ambient conditions for about 20 min. Both DOTAP and BFDMA final concentrations were 0.82 mM. We note that the charge ratio is the ratio between the negatively charged groups of the polymer (calculated in their molar concentration; according to the polymer molecular weight divided by the monomer molecular weight) and the positively charged groups of the lipids (calculated according to the molar concentration of the lipids).

In the experiments with BFDMA, the pH is about 5, while the p$K_a$ of PAA is about 4−4.5. Therefore, the charge ratio may be different than 1:1 (because some of the carboxylic acid groups may be uncharged). However, we used those conditions, because our purpose was to compare the nanostructure of the complexes with previously reported experiments that were carried out with BFDMA and DNA at the same conditions.[22]

Specimens for cryo-TEM were prepared in a controlled environment vitrification (CEVS) system at 25 °C and 100% relative humidity, as described elsewhere.[23] The vitrified specimens were examined by a FEI T12 G2 or a Philips CM 120 transmission electron microscopes with a Gatan 626, or Oxford CT-3500 cooling holders, and equilibrated in the microscopes below −178 °C. The microscopes were operated at 120 kV, in the low-dose imaging mode. A Gatan US1000 high-resolution (T12) or Gatan MultiScan 791 (CM120) cooled-CCD camera recorded the images at nominal underfocus of 1−2 $\mu$m, using the *DigitalMicrograph* software package.

Samples for DLS experiments were placed in a glass vial at 25 °C. For every system, at least five measurements were made. The DLS measurements were performed with a Bl-200SM Research Goniometer System (Brookhaven Instruments, Inc.), with a Compass 415 solid-state laser generating light of 532 nm wavelength (green). The autocorrelation was detected at 90° angle, using the CONTIN model.

The $\zeta$-potential of the solutions was characterized by a Zetasizer Nanoseries ZS (Malvern Instruments Ltd., UK), using an electric potential of 150 V. The $\zeta$-potential was calculated using the Smoluchowski relation, where the viscosity was assumed to be the same as that of water.

## RESULTS AND DISCUSSION

DOTAP is known to self-assemble into small or large unilamellar vesicles (SUV or LUV, depending on their preparation method), and when complexed with DNA, multilamellar onion-like lipoplexes.[7,11,13] Similarly, we complexed DOTAP with PAA, and characterized the nanostructure of the complexes formed. First, we observed the nanostructure of the DOTAP lipid alone. Figure 2A shows regular vesicles in the size range of 10 to 100 nm, as expected. Addition of PAA in equivalent charge ratio to the DOTAP lipid resulted in onion-like multilamellar nanostructures (asterisks, Figure 2B, D), where the negatively charged PAA is probably sandwiched between two adjacent DOTAP (lipid) bilayers.[13] Interestingly, the majority of the multilamellar onion-like structures encapsulated one or more single-walled vesicles. The DOTAP/PAA complexes are polydispersed, and probably, as in similar complex fluid systems, are not in a state of equilibrium. Arrowheads in Figure 2B−C point at onion-like nanostructures, which encapsulate two single-walled vesicles, fused together. The arrows in Figure 2C show onion-like complexes with a liquid core. In Figure 2D, the arrowhead indicates a multilamellar aggregate, in which three vesicles are encapsulated; they appear to be stacked upon each other due to two-dimensional projection of the image. The arrowhead in Figure 2E shows a multilamellar aggregate with a liquid core encapsulating a single-walled vesicle.

Another lipid that usually forms multilamellar, onion-like complexes with DNA, is the reduced form of the two-tailed ferrocene-containing cationic lipid BFDMA (Figure 1).[22] Prior to complexation of BFDMA with PAA, we characterized the lipid solution using cryo-TEM (Figure 3).


dx.doi.org/10.1021/la204095s | *Langmuir* 2012, 28, 1668−1672

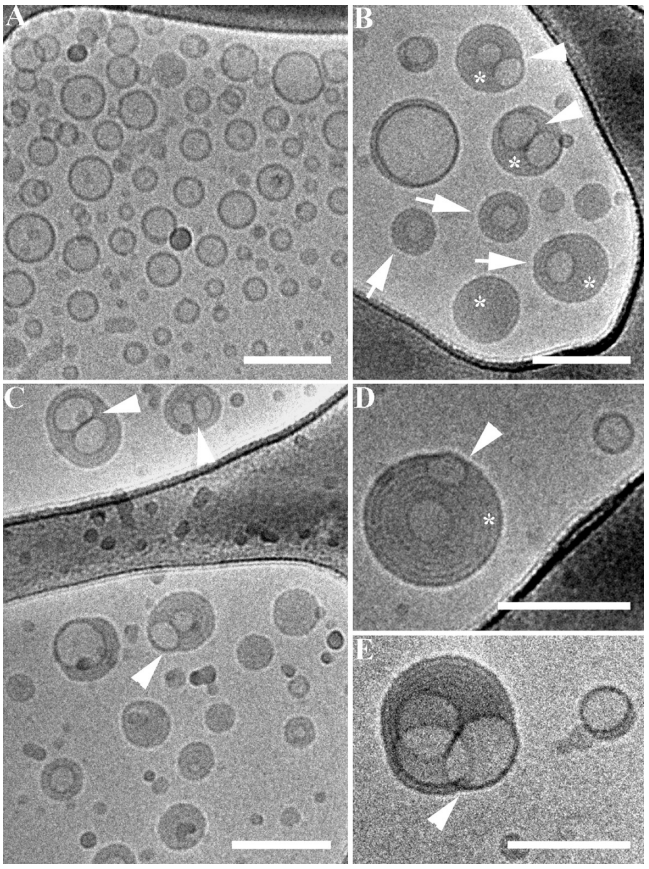


**Figure 2.** (A) 1 mM DOTAP; (B–E) DOTAP/PAA complexes at charge ratio 1; asterisks indicate multilamellar, onion-like complexes; arrows show onion-like complexes with empty cores; arrowheads point at two or more vesicles encapsulated within the onion-like complexes. Bars represent 100 nm.

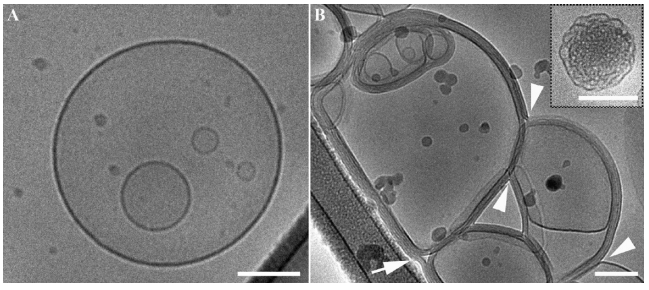


**Figure 3.** 1 mM BFDMA. (A) Regular liposome; (B) multilamellar liposomes (arrow), fused together (arrowheads), cubic-like phase (inset). Bars represent 100 nm.

The BFDMA lipid forms vesicles (Figure 3A,B) and disordered cubic-like phase (Figure 3B, inset); however, the majority of the structures are vesicles. Figure 3A shows regular vesicles; Figure 3B shows multilamellar vesicles with a few layers (indicated by an arrow), which fuse with other multilamellar vesicles (the fusion points are indicated by arrowheads). The rare disordered cubic-like nanostructure is shown in the inset in Figure 3B. These are in agreement with previous reports that the reduced form of the BFDMA lipid forms vesicles.[24,25]

Addition of PAA to the BFDMA lipid led to the formation of perfectly spherical multilamellar onion-like complexes (Figure 4). Figure 4 shows the multilamellar nanostructure of the

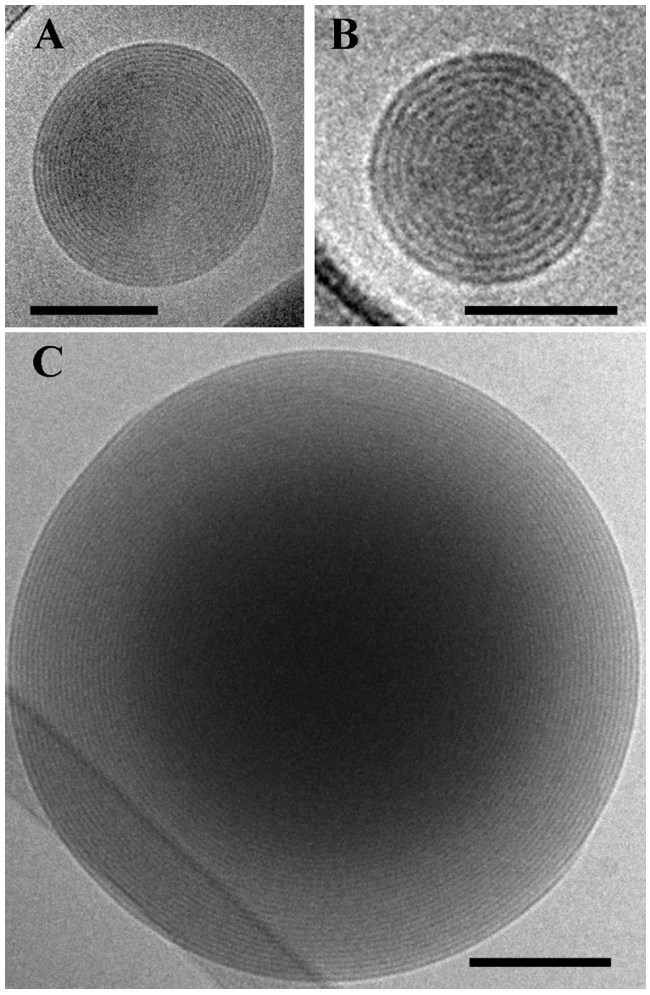


**Figure 4.** 1 mM BFDMA/PAA complexes (A–C) spherical onion-like complexes. Bars in A and C represent 100 nm, and in B 50 nm.

BFDMA/PAA complexes. Here, too, PAA is probably sandwiched between two adjacent lipid bilayers. In contrast to the DOTAP/PAA complexes, the BFDMA/PAA complexes did not exhibit liquid cores or smaller vesicles encapsulated inside the onion-like aggregate.

Cryo-TEM shows that complexes of PAA with the cationic lipids DOTAP and BFDMA at charge ratio 1 are multilamellar nanostructures, similar to the nanostructures of lipid-DNA or lipid-oligodeoxynucleotide (ODN) complexes, based on the same cationic lipids.[7,10,11,13,22] These results suggest that although PAA and nucleic acids are very different polyelectrolytes, they form similar multilamellar nanostructures with cationic lipids that are known to form lamellar nanostructures. This may imply that the self-assembly of cationic lipids and negatively charged polymers depends mostly on the electrostatic interactions, solution conditions, and on the nature of the lipid packing (i.e., whether the lipid promotes lamellar or nonlamellar structures), and less on the flexibility of the negatively charged polymer. PAA is known to be a flexible polymer with persistence length of about 1 nm.[26,27] In contrast, DNA is a semiflexible polymer with a persistence length of about 50 nm.[26,28] Also, ODNs were shown to have a persistence length close to that of PAA, about 1.3 nm.[29] We note that these numbers depend on the experimental conditions, and may change accordingly. However, the difference between those values is sufficient to emphasize the


dx.doi.org/10.1021/la204095s | *Langmuir* 2012, 28, 1668–1672

different stiffness of the polymers, and to demonstrate that those are very different polyelectrolytes.

DLS and ζ-potential measurements were employed to complete the physicochemical characterization of the complexes (Table 1). The average diameter, measured by DLS, of

**Table 1. DLS and ζ-Potential Measurements**

| | DLS (nm) | ζ-potential (mV) |
|---|---|---|
| DOTAP | 118 ± 6.4 | 60.7 ± 1.8 |
| DOTAP/PAA | 162 ± 40.3 | −49.2 ± 1.9 |
| BFDMA | NA | 45.6 ± 1.8 |
| BFDMA/PAA | 487.4 ± 143.6 | −71.1 ± 1.9 |

the DOTAP liposomes was about 120 nm. Upon addition of PAA to the DOTAP somewhat larger aggregates, about 160 nm, were formed. These results are in agreement with the cryo-TEM results, which showed polydispersity in aggregate size. However, we note that cryo-TEM is a qualitative method, which allows the observation of submicrometer aggregates that may be only a part of the whole system,[30] whereas DLS provides a quantitative measure of the aggregates size, although it emphasized the large aggregates in the population. In contrast to the DOTAP, 1 mM BFDMA forms large aggregates (several micrometers), and therefore DLS cannot provide credible results. However, from the cryo-TEM results and previous reports,[24,25] we know that reduced BFDMA forms micrometer-size aggregates. Addition of PAA to BFDMA reduced the aggregate size to an average diameter of about 500 nm (Table 1). Those measurements are in agreement with the cryo-TEM results, which showed onion-like structures in the size range of 100−600 nm (Figure 4).

ζ-potential measurements are commonly used to assess the electrostatic potential of the electrical double layer.[8,31] The ζ-potential of both DOTAP and BFDMA showed that the lipid aggregates had positive ζ-potential, while addition of PAA inverted the ζ-potential, and it became negative. The ζ-potential inversion was reported in similar cationic lipids and DNA complexes,[7,32,33] and in liposomes and oppositely charged polyelectrolytes complexes.[6,15,16] The negatively charged polymer interacts with the cationic lipids and causes inversion in the ζ-potential. In the case of an onion-like nanostructure, where the polymer is sandwiched between two adjacent lipid bilayers, the zeta potential may be negative due to oppositely charged ions that have a substantial impact on the electric double layer, or due to the outermost layer of polymer that faces the solvent. The latter scenario may happen when the concentration of the polymer is higher than the concentration of the lipid aggregates.

In summary, we have shown by cryo-TEM, DLS, and ζ-potential measurements that complexes between the oppositely charged polymer PAA and the cationic lipids DOTAP and BFDMA are similar to the structures formed between these cationic lipids and DNA (which is a very different polyelectrolyte from PAA), where the polyelectrolyte is probably sandwiched between two adjacent lipid bilayers. These results suggest that the multilamellar aggregation of liposomes and oppositely charged polyelectrolytes is energetically favorable, and may be preferred mode of aggregation for many of those systems.

## AUTHOR INFORMATION


### Corresponding Author

*Tel: +972-4-8292007; E-mail: ishi@tx.technion.ac.il.


## ACKNOWLEDGMENTS

Partial financial support was provided by the Technion Russell Berrie Nanotechnology Institute (RBNI). The microscopy work was done at the Technion Soft Matter Electron Microscopy Laboratory. We thank Professors Nicholas L. Abbott and David M. Lynn, University of Wisconsin, Madison, for useful discussions and for contributing the BFDMA lipid.

## REFERENCES


(1) Antunes, F. E.; Marques, E. F.; Miguel, M. G.; Lindman, B. *Adv. Colloid Interface Sci.* **2009**, *18*, 147−148.

(2) Bordi, F.; Sennato, S.; Truzzolillo, D. *J. Phys.: Condens. Matter* **2009**, 21.

(3) Svensson, A.; Norrman, J.; Piculell, L. *J. Phys. Chem. B* **2006**, *110*, 10332−10340.

(4) Thevenot, J.; Troutier, A. L.; Putaux, J. L.; Delair, T.; Ladaviere, C. *J. Phys. Chem. B* **2008**, *112*, 13812−13822.

(5) Vivares, E.; Ramos, L. *Langmuir* **2005**, *21*, 2185−2191.

(6) Volodkin, D.; Ball, V.; Schaaf, P.; Voegel, J. C.; Mohwald, H. *BBA-Biomembranes* **2007**, *1768*, 280−290.

(7) Koltover, I.; Salditt, T.; Safinya, C. R. *Biophys. J.* **1999**, *77*, 915−924.

(8) Ma, B.; Zhang, S.; Jiang, H.; Zhao, B.; Lv, H. *J. Controlled Release* **2007**, *123*, 184−194.

(9) Patil, S. D.; Rhodes, D. G.; Burgess, D. J. *AAPS J.* **2005**, *7*, E61−E77.

(10) Rädler, J. O.; Koltover, I.; Jamieson, A.; Salditt, T.; Safinya, C. R. *Langmuir* **1998**, *14*, 4272−4283.

(11) Simberg, D.; Weisman, S.; Talmon, Y.; Barenholz, Y. *Crit. Rev. Ther. Drug* **2004**, *21*, 257−317.

(12) Safinya, C. R. *Curr. Opin. Struct. Biol.* **2001**, *11*, 440−448.

(13) Weisman, S.; Hirsch-Lerner, D.; Barenholz, Y.; Talmon, Y. *Biophys. J.* **2004**, *87*, 609−614.

(14) Bordi, F.; Cametti, C.; Diociaiuti, M.; Gaudino, D.; Gili, T.; Sennato, S. *Langmuir* **2004**, *20*, 5214−5222.

(15) Bordi, F.; Cametti, C.; Diociaiuti, M.; Sennato, S. *Phys. Rev. E* **2005**, *71*.

(16) Bordi, F.; Cametti, C.; Sennato, S. *Chem. Phys. Lett.* **2005**, *409*, 134−138.

(17) Bordi, F.; Cametti, C.; Sennato, S.; Diociaiuti, M. *Biophys. J.* **2006**, *91*, 1513−1520.

(18) Sennato, S.; Bordi, F.; Cametti, C.; Di Biasio, A.; Diociaiuti, M. *Colloid. Surface A* **2005**, *270*, 138−147.

(19) Kilpatrick, P. K.; Miller, W. G.; Talmon, Y. *J. Colloid Interface Sci.* **1985**, *107* (1), 146−158.

(20) Talmon, Y. *J. Colloid Interface Sci.* **1983**, *93* (2), 366−382.

(21) Talmon, Y. In *Modern Characterization Methods of Surfactant Systems*; Binks, B. P., Ed.; Marcel Dekker, Inc.: New York, 1999; pp 147−178.

(22) Pizzey, C. L.; Jewell, C. M.; Hays, M. E.; Lynn, D. M.; Abbott, N. L.; Kondo, Y.; Golan, S.; Talmon, Y. *J. Phys. Chem B* **2008**, *112*, 5849−5857.

(23) Danino, D.; Bernheim-Groswasser, A.; Talmon, Y. *Colloids Surf., A* **2001**, *183*, 113−122.

(24) Kakizawa, Y.; Sakai, H.; Nishiyama, K.; Abe, M.; Shoji, H.; Kondo, Y.; Yoshino, N. *Langmuir* **1996**, *12*, 921−924.

(25) Kakizawa, Y.; Sakai, H.; Yamaguchi, A.; Kondo, Y.; Yoshino, N.; Abe, M. *Langmuir* **2001**, *17*, 8044−8048.

(26) Krishnaswamy, R.; Mitra, P.; Raghunathan, V. A.; Sood, A. K. *Europhys. Lett.* **2003**, *62*, 357−362.

(27) Walczak, W. J.; Hoagland, D. A.; Hsu, S. L. *Macromolecules* **1992**, *25*, 7317−7323.

(28) Dobrynin, A. V. *Macromolecules* **2006**, *39*, 9519−9527.

(29) Schalhorn, K. A.; Freedman, K. O.; Moore, J. M. *Appl. Phys. Lett.* **2005**, *87*, 033901−1−3.
(30) De Smet, Y.; Danino, D.; Deriemaeker, L.; Talmon, Y.; Finsy, R. *Langmuir* **2000**, *16*, 961−967.
(31) Egorova, E. M. *Electrophoresis* **1994**, *15*, 1125−1131.
(32) Hays, M. E.; Jewell, C. M.; Kondo, Y.; Lynn, D. M.; Abbott, N. L. L. *Biophys. J.* **2007**, *93*, 4414−4424.
(33) Hirsch-Lerner, D.; Zhang, M.; Eliyahu, H.; Ferrari, M. E.; Wheeler, C. J.; Barenholz, Y. *Biochim. Biophys. Acta* **2005**, *1714*, 71−84.